Mathematics Faculty Publications   Department of Mathematics

2017

AN OPTIMAL A POSTERIORI ERROR ESTIMATES OF THE LOCAL DISCONTINUOUS GALERKIN METHOD FOR THE SECOND-ORDER WAVE EQUATION IN ONE SPACE DIMENSION

Mahboub Baccouch
University of Nebraska at Omaha, mbaccouch@unomaha.edu

Follow this and additional works at: https://digitalcommons.unomaha.edu/mathfacpub

Part of the Mathematics Commons

Please take our feedback survey at: https://unomaha.az1.qualtrics.com/jfe/form/ SV_8cchtFmpDyGfBLE

AN OPTIMAL *A POSTERIORI* ERROR ESTIMATES OF THE LOCAL DISCONTINUOUS GALERKIN METHOD FOR THE SECOND-ORDER WAVE EQUATION IN ONE SPACE DIMENSION

MAHBOUB BACCOUCH

Abstract. In this paper, we provide the optimal convergence rate of *a posteriori* error estimates for the local discontinuous Galerkin (LDG) method for the second-order wave equation in one space dimension. One of the key ingredients in our analysis is the recent optimal superconvergence result in [W. Cao, D. Li and Z. Zhang, *Commun. Comput. Phys.* 21 (1) (2017) 211-236]. We first prove that the LDG solution and its spatial derivative, respectively, converge in the L^2-norm to $(p + 1)$-degree right and left Radau interpolating polynomials under mesh refinement. The order of convergence is proved to be $p + 2$, when piecewise polynomials of degree at most p are used. We use these results to show that the leading error terms on each element for the solution and its derivative are proportional to $(p + 1)$-degree right and left Radau polynomials. These new results enable us to construct residual-based *a posteriori* error estimates of the spatial errors. We further prove that, for smooth solutions, these *a posteriori* LDG error estimates converge, at a fixed time, to the true spatial errors in the L^2-norm at $\mathcal{O}(h^{p+2})$ rate. Finally, we show that the global effectivity indices in the L^2-norm converge to unity at $\mathcal{O}(h)$ rate. The current results improve upon our previously published work in which the order of convergence for the *a posteriori* error estimates and the global effectivity index are proved to be $p+3/2$ and $1/2$, respectively. Our proofs are valid for arbitrary regular meshes using P^p polynomials with $p \geq 1$. Several numerical experiments are performed to validate the theoretical results.

Key words. Local discontinuous Galerkin method, second-order wave equation, superconvergence, Radau points, *a posteriori* error estimation.

1. Introduction

In this paper, we analyze a residual-based *a posteriori* error estimates of the spatial errors for the semi-discrete local discontinuous Galerkin (LDG) method applied to the following one-dimensional linear wave equation

$$\text{(1a)} \qquad u_{tt} = u_{xx} + cu, \quad x \in [a, b], \ t \in [0, T],$$

subject to the initial and periodic boundary conditions

$$\text{(1b)} \qquad u(x, 0) = g(x), \quad u_t(x, 0) = h(x), \quad x \in [a, b],$$

$$\text{(1c)} \qquad u(a, t) = u(b, t), \quad u_x(a, t) = u_x(b, t), \quad t \in [0, T],$$

where c is assumed to be a constant. For the sake of simplicity, we only consider the case of periodic boundary conditions. However, this assumption is not essential. We note that if other boundary conditions (*e.g.*, Dirichlet or Neumann or mixed boundary conditions) are chosen, the LDG method can be easily designed; see [6, 10, 19, 39] for some discussion. In our analysis, the initial conditions are assumed to be sufficiently smooth functions so that the exact solution, $u(x, t)$, is a smooth function on $[a, b] \times [0, T]$.

The discontinuous Galerkin (DG) method was first developed in the early 1970s by Reed and Hill [34] for solving hyperbolic conservation laws containing only first order spatial derivatives. However, in the last two decades it has become attractive as a powerful simulation tool for solving many partial differential equations. The DG method is a class of finite element methods, using discontinuous, piecewise polynomials as the numerical solution and the test functions. The DG method combines the best proprieties of the classical continuous finite element and finite volume methods such as consistency, flexibility, stability, conservation of local physical quantities, robustness and compactness. Recently, DG methods become highly attractive and popular, mainly because these methods are high-order accurate, nonlinear stable, highly parallelizable, easy to handle complicated geometries and boundary conditions, and capable to capture discontinuities without spurious oscillations. Since then the DG method has been analyzed and extended to a wide range of applications. In particular, for time dependent problems, Cockburn and Shu [26] extended the DG method to solve first-order hyperbolic partial differential equations of conservation laws. They used a method of lines which consists of applying the DG scheme to approximate the problem in space and then to apply a Runge-Kutta scheme in time to obtain an RKDG scheme. They further developed the local DG (LDG) method for convection-diffusion problems [27]. The proceeding of Shu [36] contain a more complete and current survey of the DG method and its applications.

The LDG method we discuss in this paper is an extension of the DG method aimed at solving differential equations containing higher than first-order spatial derivatives. The LDG method for solving convection-diffusion problems was first introduced by Cockburn and Shu in [27]. LDG methods are robust and high-order accurate, can achieve stability without slope limiters, and are locally (elementwise) mass-conservative. This last property is very useful in the area of computational fluid dynamics, especially in situations where there are shocks, steep gradients or boundary layers. Moreover, LDG methods are extremely flexible in the mesh-design; they can easily handle meshes with hanging nodes, elements of various types and shapes, and local spaces of different orders. They further exhibit strong superconvergence that can be used to estimate the discretization errors. LDG schemes have been successfully applied to hyperbolic, elliptic, and parabolic partial differential equations [6, 26, 28, 29, 19, 38, 33, 27, 15, 18, 19, 7, 2, 17, 3, 4], to mention a few. A review of the LDG methods is given in [7, 11, 17, 25, 23, 16, 24, 19, 37, 39, 14].

In [6], we investigated the superconvergence properties of the LDG method for the second-order wave equation in one space dimension. We performed an error analysis on one element and showed that the p-degree LDG solution and its spatial derivative are $\mathcal{O}(h^{p+2})$ superconvergent at the roots of $(p+1)$-degree right and left Radau polynomials, respectively. Computational results showed that global superconvergence holds for LDG solutions. We used these results to construct asymptotically correct *a posteriori* error estimates by solving local steady problem with no boundary conditions on each element. However, we only presented several numerical results suggesting that the global spatial error estimates converge to the true errors under mesh refinement where temporal errors are assumed to be negligible. In [10], we analyzed the LDG method introduced by the author in [6] for solving the one-dimensional second-order wave equation. We used a suitable projection of the initial conditions for the numerical scheme and proved optimal L^2

error estimates for the LDG solution and its spatial derivative. We also proved that the LDG solution and its derivative are $\mathcal{O}(h^{p+3/2})$ super close to special projections of the true solutions. Moreover, we showed that the true errors can be divided into significant and less significant parts. The significant parts of the discretization errors for the LDG solution and its spatial derivative are proportional to $(p+1)$-degree right and left Radau polynomials, respectively. In [12], we applied the superconvergence results of Baccouch [10] to prove that the implicit residual-based *a posteriori* error estimates of Baccouch [6] converge to the true spatial errors at $\mathcal{O}(h^{p+3/2})$ rate. Our computational results indicate that the observed numerical convergence rates are higher than the theoretical rates.

More recently, Cao *et al.* [13] studied the superconvergence properties of the LDG method for the one-dimensional linear wave equation $u_{tt} = u_{xx} + cu$ subject to some appropriate initial and boundary conditions, when the alternating flux is used. They used suitable initial discretizations to show that the numerical trace of the LDG approximation at nodes, as well as the cell average, converge with an order $2p+1$. In addition, they established $(p+2)$-th order and $(p+1)$-th order superconvergence rates for the function value error and the derivative error at Radau points, respectively. They also proved that the LDG solution is superconvergent with an order $p+2$ towards a special Gauss-Radau projection of the exact solution. Their analysis is valid for arbitrary regular meshes and for P^p polynomials with arbitrary $p \geq 1$. They performed numerical experiments to demonstrate that the superconvergence rates are optimal. The results in the current paper depend heavily on results from the references [13].

In this paper, we analyze the global convergence of an implicit residual-based *a posteriori* error estimates for the LDG method applied to one-dimensional linear second-order wave equation. We first apply the recent optimal superconvergence results [13] to prove that, for smooth solutions, the true errors can be divided into significant and less significant parts. The significant parts of the discretization errors for the LDG solution and its spatial derivative are proportional to $(p+1)$-degree right and left Radau polynomials, respectively, when p-degree piecewise polynomials with $p \geq 1$ are used. The less significant parts converge to zero at a rate of $p+2$. Superconvergence toward right and left Radau interpolating polynomials are used to prove that our *a posteriori* LDG error estimates for the solution and its spatial derivative, at any fixed time, converge to the true spatial errors in the L^2-norm under mesh refinement. The order of convergence is proved to be $p+2$. Consequently, by adding the error estimates to the LDG solutions only once at the end of the computation, we show that the post-processed approximations converge to the exact solutions at $\mathcal{O}(h^{p+2})$ rate in the L^2-norm. Finally, we prove that the global effectivity indices, for both the solution and its derivative, in the L^2-norm converge to unity at $\mathcal{O}(h)$. Our results are valid for arbitrary regular meshes and schemes with $p \geq 1$. These results improve upon our previously published work [12] in which the order of convergence in the L^2-norm for the *a posteriori* error estimates and the global effectivity indices are proved to be $p+3/2$ and $1/2$, respectively. Our analysis is valid for arbitrary regular meshes and for P^p polynomials with arbitrary $p \geq 1$. To the best knowledge of the author, our results are novel in the current available literature.

This paper is organized as follows: In section 2, we recall the LDG scheme for solving (1) and present some recent superconvergence results which will be needed in our

a posteriori error analysis. In section 3, we present new optimal superconvergence results toward Radau interpolating polynomials. Section 4 is the main body of the paper, where we present our *a posteriori* error estimation procedure and prove that these error estimates converge to the true errors under mesh refinement in L^2-norm with optimal convergence rate. In section 5, we present several numerical examples to demonstrate the asymptotic exactness of the *a posteriori* error estimates under mesh refinement in L^2-norm. We conclude and discuss our results in section 6.

2. The LDG scheme and preliminary results

Here, we present the LDG scheme for solving (1). We follow the method in [13, 12] and mostly use the notation therein. We divide the computational domain $\Omega = [a, b]$ into N intervals $I_i = [x_{i-1}, x_i]$, $i = 1, \ldots, N$, where $a = x_0 < x_1 < \cdots < x_N = b$. Let $h_i = x_i - x_{i-1}$ be the length of the interval I_i, and denote $h = \max\limits_{1 \le i \le N} h_i$ and $h_{min} = \min\limits_{1 \le i \le N} h_i$ to be the lengths of the largest and smallest intervals, respectively. In this paper, we consider regular meshes, that is $h \le K h_{min}$, where $K \ge 1$ is a constant during mesh refinement. For simplicity, we use $v\big|_i$ to denote the value of the continuous function $v = v(x, t)$ at $x = x_i$. We also use $v^-\big|_i$ and $v^+\big|_i$ to denote the left limit and the right limit of v at the discontinuity point x_i, i.e.,

$$v^-\big|_i = v(x_i^-, t) = \lim_{s \to 0^-} v(x_i + s, t), \qquad v^+\big|_i = v(x_i^+, t) = \lim_{s \to 0^+} v(x_i + s, t).$$

The finite element space is defined as $V_h^p = \{v : v|_{I_i} \in P^p(I_i), \ i = 1, \ldots, N\}$, where $P^p(I_i)$ is the space of polynomials of degree at most p on I_i with coefficients as functions of t. Note that polynomials in the space V_h^p are allowed to have discontinuities across element boundaries.

To construct the LDG scheme, we introduce an auxiliary variable $q = u_x$ and rewrite the equation (1a) as a first-order linear system

$$(2) \qquad\qquad u_{tt} - cu - q_x = 0, \qquad q - u_x = 0.$$

The semi-discrete LDG scheme we consider consists of finding $u_h(\cdot, t) \in V_h^p$ and $q_h(\cdot, t) \in V_h^p$ such that for any $v, w \in V_h^p$ and for all $i = 1, \ldots, N$,

$$(3a) \qquad \int_{I_i} ((u_h)_{tt} - cu_h)\, v\, dx + \int_{I_i} q_h v_x dx - \hat{q}_h v^-\big|_i + \hat{q}_h v^+\big|_{i-1} = 0,$$

$$(3b) \qquad \int_{I_i} q_h w\, dx + \int_{I_i} u_h w_x dx - \hat{u}_h w^-\big|_i + \hat{u}_h w^+\big|_{i-1} = 0,$$

where, the so-called numerical fluxes $\hat{u}_h$ and $\hat{q}_h$ are the discrete approximations to the traces of u and q at the nodes. To achieve global superconvergence results, the discrete initial conditions $u_h(x, 0) \in V_h^p$ and $(u_h)_t(x, 0) \in V_h^p$ must be carefully designed as

$$(3c) \qquad\qquad u_h(x, 0) = u_I^l(x, 0), \quad (u_h)_t(x, 0) = (u_I^l)_t(x, 0),$$

where u_I^l is a special interpolation function which will be defined later. These special initial conditions are designed to better control the initial errors. The exact implementation of the initial condition will be described later and it can be found in [13].

To complete the definition of the LDG scheme, we still need to define $\hat{u}_h$ and $\hat{q}_h$ on the boundaries of I_i. We would like to mention that the numerical fluxes have to be suitably chosen in order to ensure the stability of the method and also to improve

the order of convergence. For the periodic boundary conditions, we consider the alternating fluxes (*e.g.*, see [13, 12]) *i.e.*,

$$(3d) \qquad \hat{u}_h\big|_i = u_h^-\big|_i, \qquad \hat{q}_h\big|_i = q_h^+\big|_i, \qquad i = 0, \dots, N.$$

Even though we only consider the case of periodic boundary conditions, this assumption is not essential, since we do not use Fourier analysis. We note that if other boundary conditions are chosen, the numerical fluxes can be easily designed; see *e.g.*, [6, 10, 12, 18]. For instance, the numerical fluxes associated with the mixed boundary conditions of the form $u(a,t) = u_1(t)$ and $u_x(b,t) = u_2(t)$ can be taken as

$$\hat{u}_h\big|_i = \begin{cases} u_1, & i = 0, \\ u_h^-\big|_i, & i = 1, \dots, N, \end{cases} \quad , \quad \hat{q}_h\big|_i = \begin{cases} q_h^+\big|_i, & i = 0, \dots, N-1, \\ u_2, & i = N. \end{cases}$$

Similarly, the numerical fluxes associated with the boundary conditions $u_x(a,t) = u_1(t)$ and $u(b,t) = u_2(t)$ can be easily designed. For the Dirichlet boundary conditions, we use the so-called the minimal dissipation LDG (md-LDG) method; see, *e.g.*, [17, 18, 6, 12, 7, 9, 8]. More precisely, the numerical fluxes associated with the Dirichlet boundary conditions of the form $u(a,t) = u_1(t)$ and $u(b,t) = u_2(t)$ can be taken as

$$\hat{u}_h\big|_i = \begin{cases} u_1, & i = 0, \\ u_h^-\big|_i, & i = 1, \dots, N-1, \\ u_2, & i = N, \end{cases} \quad \hat{q}_h\big|_i = \begin{cases} q_h^+\big|_i, & i = 0, \dots, N-1, \\ \left(q_h^- - \delta(u_h^- - u_2)\right)\big|_i, & i = N. \end{cases}$$

where the stabilization parameter δ for the LDG method is given by $\delta = \frac{p}{h_i}$. The distinctive feature of the md-LDG method is that the stabilization parameter associated with the numerical trace of q is taken to be identically zero on all interior nodes (only the numerical flux at boundary $x = b$ is penalized) and this is why its dissipation is said to be minimal.

2.1. Norms, projections, and properties of the finite element space.
Throughout the paper, we adopt the standard notation for Sobolev spaces and their associated norms. Denote $\|u\|_{p,D}$ to be the standard L^p-norm of u on D with $1 \le p < \infty$. When $D = \Omega$, we omit the index D, and if $p = 2$, we set $\|u\|_{2,D} = \|u\|_D$. We also use $\|u\|$ to denote $\|u\|_{2,\Omega}$. Moreover, the standard L^∞-norm of u on D is defined by $\|u\|_{\infty,D} = \sup\limits_{(x,y) \in D} |u|$.

The Sobolev spaces $W^{s,p}(D)$ with $1 \le p \le \infty$ on a domain $D \subset \Omega$ consists of functions that have generalized derivatives of order s in the space $L^p(D)$, *i.e.*, $W^{s,p}(D) = \{u : \partial_x^k u \in L^p(D), \ \forall \ k = 0, \dots, s\}$. The norm of $W^{s,p}(D)$ is defined by $\|u\|_{s,p,D} = \left(\sum_{k=0}^s \|\partial_x^k u\|_{p,D}^p\right)^{1/p}$ with the standard modification for $p = \infty$. We shall also use the following notation for the semi-norm $|u|_{s,p,D} = \left(\|\partial_x^s u\|_{p,D}^p\right)^{1/p}$. For $p = 2$ and $s \ge 1$, we set $W^{s,2}(D) = H^s(D)$, $\|u\|_{s,2,D} = \|u\|_{s,D}$, and $|u|_{s,2,D} = |u|_{s,D}$. Finally, we define the semi-norm and norm on the whole computational domain Ω as

$$|u|_{s,p,\Omega} = \left(\sum_{i=1}^N |u|_{s,p,I_i}^p\right)^{1/p}, \qquad \|u\|_{s,p,\Omega} = \left(\sum_{i=1}^N \|u\|_{s,p,I_i}^p\right)^{1/p}.$$

In order to simplify the notation, we drop the domain from the norms and semi-norms subscript, if the domain is $D = \Omega$. Finally, we use $\|u(t)\|$ to denote the value

of $\|u(\cdot,t)\|$ at time t. Throughout the paper, we omit the argument t and we use $\|u\|$ to denote $\|u(t)\|$ whenever confusion is unlikely.

For $p \geq 1$, we define $P_h^{\pm}u$ as two special Gauss-Radau projections of u into V_h^p as follows [19]: The restrictions of P_h^+u and P_h^-u to I_i are polynomials in $P^p(I_i)$ satisfying

(4) $\displaystyle\int_{I_i} (P_h^-u - u)v\,dx = 0, \ \forall \ v \in P^{p-1}(I_i), \quad \text{and} \quad (P_h^-u - u)^-\big|_i = 0,$

(5) $\displaystyle\int_{I_i} (P_h^+u - u)v\,dx = 0, \ \forall \ v \in P^{p-1}(I_i), \quad \text{and} \quad (P_h^+u - u)^+\big|_{i-1} = 0.$

These special projections are used in the error estimates of the DG methods to derive optimal L^2 error bounds in the literature, *e.g.*, in [19]. They are mainly used to eliminate the jump terms at the element boundaries in the error estimates in order to prove the optimal L^2 error estimates. In our analysis, we need the following projection results [20]: If $u \in H^{p+1}(I_i)$, then there exists a positive constant C independent of the mesh size h, such that

(6) $\left\| u - P_h^{\pm}u \right\|_{I_i} + h_i \left\| (u - P_h^{\pm}u)_x \right\|_{I_i} \leq Ch_i^{p+1} |u|_{p+1,I_i}.$

Finally, we state some inverse properties of the finite element space V_h^p [33]: For any $v \in P^p(I_i)$, there exists a positive constant C independent of v and h, such that

$$\|v_x\|_{I_i} \leq Ch_i^{-1} \|v\|_{I_i}, \quad \|v\|_{\infty,I_i} \leq Ch_i^{-1/2} \|v\|_{I_i}, \quad \left|v^+|_{i-1}\right| + \left|v^-|_i\right| \leq Ch_i^{-1/2} \|v\|_{I_i}.$$

In the rest of the paper, we will not differentiate between various constants, and instead will use a generic constant C to represent a positive constant independent of the mesh size h, but which may depend upon the exact smooth solution of the partial differential equation (1a) and its derivatives.

2.2. Legendre and Radau polynomials. In our analysis, we need some properties of Radau polynomials. We denote by $\tilde{L}_p$ the Legendre polynomial of degree p on $[-1,1]$, which can be defined by the Rodrigues formula [1]

(7a) $\displaystyle\tilde{L}_p(\xi) = \frac{1}{2^p p!} \frac{d^p}{d\xi^p}[(\xi^2 - 1)^p], \quad -1 \leq \xi \leq 1.$

The Legendre polynomial satisfies the following properties: $\tilde{L}_p(1) = 1$, $\tilde{L}_p(-1) = (-1)^p$, and

(7b) $\displaystyle\int_{-1}^{1} \tilde{L}_p(\xi)\tilde{L}_q(\xi)\,d\xi = \frac{2}{2p+1}\delta_{pq}, \quad$ where δ_{pq} is the Kronecker symbol.

We note that the $(p+1)$-degree Legendre polynomial on $[-1,1]$ can be written as

$$\tilde{L}_{p+1}(\xi) = \frac{(2p+2)!}{2^{p+1}[(p+1)!]^2}\xi^{p+1} + \tilde{q}_p(\xi), \quad \text{where } \tilde{q}_p \in P^p([-1,1]).$$

Next, we define the $(p+1)$-degree right, $\tilde{R}_{p+1}^-$, and left, $\tilde{R}_{p+1}^+$, Radau polynomials on $[-1,1]$ as

(8) $\tilde{R}_{p+1}^-(\xi) = \tilde{L}_{p+1}(\xi) - \tilde{L}_p(\xi), \quad \tilde{R}_{p+1}^+(\xi) = \tilde{L}_{p+1}(\xi) + \tilde{L}_p(\xi), \quad -1 \leq \xi \leq 1.$

The $(p+1)$-degree right and left Radau polynomials on $[-1,1]$ have $p+1$ real distinct roots $-1 < \xi_0^- < \cdots < \xi_p^- = 1$ and $-1 = \xi_0^+ < \cdots < \xi_p^+ < 1$, respectively.

Mapping the physical element I_i into the reference element I by the standard affine mapping

$$(9) \qquad x(\xi, h_i) = \frac{x_i + x_{i-1}}{2} + \frac{h_i}{2}\xi,$$

we obtain the p-degree shifted Legendre and Radau polynomials on I_i:

$$L_{p,i}(x) = \tilde{L}_p\left(\frac{2x - x_i - x_{i-1}}{h_i}\right), \quad R_{p,i}(x) = \tilde{R}_p\left(\frac{2x - x_i - x_{i-1}}{h_i}\right).$$

The roots of $R_{p+1,i}^{\pm}(x)$, $x \in I_i$ are defined by $x_{i,j}^{\pm} = \frac{x_i + x_{i-1}}{2} + \frac{h_i}{2}\xi_j^{\pm}$, $j = 0, 1, \ldots, p$. Next, we define the monic Radau polynomials, $\psi_{p+1,i}^{\pm}(x)$, on I_i as

$$(10)$$

$$\psi_{p+1,i}^{\pm}(x) = \frac{((p+1)!)^2}{(2p+2)!}h_i^{p+1}R_{p+1,i}^{\pm}(x) = c_p h_i^{p+1} R_{p+1,i}^{\pm}(x), \quad \text{where } c_p = \frac{((p+1)!)^2}{(2p+2)!}.$$

In the next lemma, we recall some results which will be needed in our *a posteriori* error analysis.

Lemma 2.1. *The $(p+1)$-degree monic Radau polynomials on I_i, $\psi_{p+1,i}^{\pm}$, satisfy the properties*

$$(11) \qquad \left\|\psi_{p+1,i}^+\right\|_{I_i}^2 = \left\|\psi_{p+1,i}^-\right\|_{I_i}^2 = \frac{2(2p+2)}{(2p+1)(2p+3)}c_p^2 h_i^{2p+3},$$

where $c_p = \frac{[(p+1)!]^2}{(2p+2)!}$.

Proof. The proof of this lemma can be found in [7], more precisely in its Lemma 2.1. □

2.3. Preliminary results. In [13], the authors analyzed the same LDG method described at the beginning of section 2. They selected suitable initial discretizations for the LDG scheme and proved the $(2p+1)$-th order superconvergence rate of the LDG approximation at the downwind points and for the cell averages. They further proved that the function value approximation and the derivative approximation are superconvergent with orders $p+2$ and $p+1$ at Radau points, respectively. Finally, they proved that the LDG solutions u_h and q_h are superconvergent with an order $p+2$ toward the special Gauss-Radau projections of the exact solutions $P_h^- u$ and $P_h^+ q$, respectively. We briefly review some of their results which are needed in our *a posteriori* error analysis.

To begin, we note that the suitable initial conditions are designed as follows [13]

$$(12a) \qquad u_h(x, 0) \;=\; u_I^l(x, 0) = P_h^- u(x, 0) - w_u^l(x, 0),$$

$$(12b) \qquad (u_h)_t(x, 0) \;=\; \partial_t u_I^l(x, 0) = P_h^- u_t(x, 0) - \partial_t w_u^l(x, 0),$$

where w_u^l is a suitable correction function. It is defined in section 3.2 of [13] (see its Eq. (3.14) and Eq. (3.15)). For the sake of completeness, we recall the definition of w_u^l. First, we define, for any function $v(s) \in L^1[a, b]$, an integral operator D^{-1} by

$$D_s^{-1}v(x) = \frac{1}{\bar{h}_i}\int_{x_{i-1}}^x v(y)dy = \int_{-1}^s \tilde{v}(\xi)d\xi, \quad x \in I_i, \quad i = 1, \ldots, N,$$

where $\bar{h}_i = h_i/2 = (x_i - x_{i-1})/2$, $s = (x - \bar{x}_i)/h_i \in [-1, 1]$, $\bar{x}_i = (x_i + x_{i-1})/2$, $\tilde{v}(s) = v(x)$.

Next, we define a class of special functions, which are used to construct the correction function w_u^l

$$F_{1,1}(x) = P_h^+ D_s^{-1} L_{p,i}(x), \quad F_{1,k}(x) = P_h^+ D_s^{-1} F_{2,k-1}(x), \quad k = 2, \ldots, p, \quad x \in I_i,$$

$$F_{2,1}(x) = P_h^- D_s^{-1} L_{p,i}(x), \quad F_{2,k}(x) = P_h^- D_s^{-1} F_{1,k-1}(x), \quad k = 2, \ldots, p, \quad x \in I_i,$$

where $L_{p,i}(x)$ denotes the Legendre polynomial of degree p on I_i.

Suppose $u(x,t)$ and $q(x,t)$, for $x \in I_i$, have the following Legendre expansions,

$$u(x,t) = \sum_{k=0}^{\infty} u_{k,i}(t) L_{k,i}(x), \qquad u_{k,i}(t) = \frac{2k+1}{h_i} \int_{I_i} u(x,t) L_{k,i}(x) dx,$$

$$q(x,t) = \sum_{k=0}^{\infty} q_{k,i}(t) L_{k,i}(x), \qquad q_{k,i}(t) = \frac{2k+1}{h_i} \int_{I_i} q(x,t) L_{k,i}(x) dx.$$

Then, by the definitions of $P_h^- u$ and $P_h^+ q$, we have

$$P_h^- u(x,t) = -\bar{u}_{p,i}(t) L_{p,i}(x) + \sum_{k=0}^{p} u_{k,i}(t) L_{k,i}(x),$$

$$P_h^+ q(x,t) = -\tilde{q}_{p,i}(t) L_{p,i}(x) + \sum_{k=0}^{p} q_{k,i}(t) L_{k,i}(x),$$

where

$$\bar{u}_{p,i}(t) = -u(x_i^-, t) + \sum_{k=0}^{p} u_{k,i}(t) = -u(x_i^-, t) + \sum_{k=0}^{p} \frac{2k+1}{h_i} \int_{I_i} u(x,t) L_{k,i}(x) dx,$$

$$\tilde{q}_{p,i}(t) = (-1)^{p+1} q(x_{i-1}^+, t) + \sum_{k=0}^{p} (-1)^{p+k} q_{k,i}(t)$$

$$= (-1)^{p+1} q(x_{i-1}^+, t) + \sum_{k=0}^{p} (-1)^{p+k} \frac{2k+1}{h_i} \int_{I_i} q(x,t) L_{k,i}(x) dx.$$

We also define the following function

$$G_1 = \tilde{q}_{p,i}, \quad Q_1 = (\partial_t^2 - c)\bar{u}_{p,i}, \quad G_k = Q_{k-1}, \quad Q_k = (\partial_t^2 - c)G_{k-1}, \quad k \geq 2.$$

Then for any given l, $1 \leq l \leq p$, we define correction functions in each element I_i, $i = 1, \ldots, N$ as

$$w_u^l(x,t) = \sum_{k=1}^{l} (\bar{h}_i)^k G_k(t) F_{2,k}(x), \quad w_q^l(x,t) = \sum_{k=1}^{l} (\bar{h}_i)^k Q_k(t) F_{1,k}(x).$$

With the correction functions w_u^l and w_q^l with $1 \leq l \leq p$, we define the special interpolation functions

$$u_I^l = P_h^- u - w_u^l, \quad q_I^l = P_h^+ q - w_q^l.$$

Next, we recall the following important superconvergence result from [13]. This result will be used in our analysis.

Theorem 1. *Let* $u \in W^{p+4,\infty}(\Omega)$, $\partial_t u \in W^{p+3,\infty}(\Omega)$, *and* (u_h, q_h) *be the LDG solution of (3) with the initial conditions defined by (12) with $l = 1$. Then there exists a positive constant C independent of h such that, $\forall\, t \in [0, T]$,*

$$(13) \qquad \|u_h - P_h^- u\| + \|q_h - P_h^+ q\| \leq C h^{p+2} \left(\|u\|_{p+4,\infty} + \|\partial_t u\|_{p+3,\infty} \right).$$

Proof. Cf. [13]. More precisely, the estimate (13) can be found in its Corollary 3.1. □

Remark 2.1. The estimate (13) indicates that u_h and q_h are $\mathcal{O}(h^{p+2})$ super close to the Gauss-Radau projections $P_h^- u$ and $P_h^+ q$, respectively.

Remark 2.2. In this paper, we apply the superconvergence result (13) to prove our *a posteriori* LDG error estimates converge, at a fixed time, to the true spatial errors in the L^2-norm at $\mathcal{O}(h^{p+2})$ rate. Our theoretical results are valid if we choose the initial values defined by (12) with $l = 1$. However, our numerical experiments indicate that these suitable initial values are only needed in the analysis. Actually, we have observed similar results in our numerical experiments when using the initial values $u_h(x, 0) = P_h^- u(x, 0)$ and $(u_h)_t(x, 0) = P_h^- u_t(x, 0)$; see numerical experiments in [10, 12].

Denote the errors between the exact solutions of (2) and the numerical solutions defined in (3) to be $e_u = u - u_h$ and $e_q = q - q_h$. Following the standard technique in finite element analysis, we split the actual errors into two parts

$$(14) \qquad e_u = \epsilon_u + \bar{e}_u, \quad e_q = \epsilon_q + \bar{e}_q,$$

where $\epsilon_u = u - P_h^- u$ and $\epsilon_q = q - P_h^+ q$ are the projection errors and $\bar{e}_u = P_h^- u - u_h$ and $\bar{e}_q = P_h^+ q - q_h$ are the errors between the numerical solutions and the projection of the exact solutions.

For the sake of completeness, we include the following results from [10] which will be needed in our *a posteriori* error analysis.

Theorem 2. *Under the assumptions of Theorem 1, there exists a positive constant C independent of h such that,*

$$(15) \qquad \|e_u\| \quad \leq \quad C\, h^{p+1}, \quad \forall\, t \in [0, T].$$
$$(16) \qquad \|e_q\| \quad \leq \quad C\, h^{p+1}, \quad \forall\, t \in [0, T].$$
$$(17) \qquad \|(e_u)_{tt}\| \quad \leq \quad C\, h^{p+1}, \quad \forall\, t \in [0, T].$$

Proof. Cf. [10]. More precisely, the estimate (15) can be found in its Corollary 3.1. The the estimates (16) and (17) can be found in its Theorem 3.1. We note that the estimates (15) and (16) can also be deduced from (13) and (6). □

In the next corollary, we prove some optimal L^2 error estimates which will be needed for our *a posteriori* error analysis.

Corollary 2.1. *Under the assumptions of Corollary 1, there exists a constant C such that*

$$(18) \qquad \|e_u\|_1 \leq Ch^p, \qquad \|e_q\|_1 \leq Ch^p.$$

Proof. The proof follows from (14), the triangle inequality, the standard inverse inequality, the projection result (6), and the estimate (13). Therefore the details are omitted. □

Now, we are ready to prove the optimal superconvergence rate toward Radau interpolating polynomials.

3. Superconvergence toward Radau interpolating polynomials

First, we define four interpolation operators $\pi^{\pm}$ and $\hat{\pi}^{\pm}$ [10]. The projection π^{-} is defined as follows: For any function u, $\pi^{-}u\big|_{I_i} \in P^p(I_i)$ and interpolates u at the roots of the $(p+1)$-degree right Radau polynomial shifted to I_i, $x_{i,j}^{-}, j = 0, 1, \ldots, p$. Similarly, $\pi^{+}u\big|_{I_i} \in P^p(I_i)$ and interpolates u at $x_{i,j}^{+}, j = 0, 1, \ldots, p$. Next, the interpolation operators $\hat{\pi}^{\pm}$ are such that $\hat{\pi}^{\pm}u\big|_{I_i} \in P^{p+1}(I_i)$ and are defined as follows: $\hat{\pi}^{-}u\big|_{I_i}$ interpolates u at $x_{i,j}^{-}, j = 0, 1, \ldots, p$, and at an additional point $\bar{x}_i^{-}$ in I_i with $\bar{x}_i^{-} \neq x_{i,j}^{-}, j = 0, 1, \ldots, p$. Similarly, $\hat{\pi}^{+}u\big|_{I_i}$ interpolates u at $x_{i,j}^{+}, j = 0, 1, \ldots, p$, and at an additional point $\bar{x}_i^{+}$ in I_i with $\bar{x}_i^{+} \neq x_{i,j}^{+}, j = 0, 1, \ldots, p$.

Remark 3.1. We would like to mention that the operators $\hat{\pi}^{\pm}$ are only needed for technical purposes in the proof of the error estimates. We also would like to emphasize that the polynomials $\hat{\pi}^{\pm}u$ depend on the additional points $\bar{x}_i^{\pm}$. For clarity of presentation, we choose the two additional points $\bar{x}_i^{\pm}$ on each element $I_i = [x_{i-1}, x_i]$ as as follows: $\bar{x}_i^{-} = x_{i-1}$ (left-end point of I_i) and $\bar{x}_i^{+} = x_i$ (right-end point of I_i). We note that $\bar{x}_i^{-} \neq x_{i,j}^{-}, j = 0, 1, \ldots, p$ and $\bar{x}_i^{+} \neq x_{i,j}^{+}, j = 0, 1, \ldots, p$. Moreover, we can easily verify that $\hat{\pi}^{\pm}u$ are given by

$$(19) \qquad\qquad \hat{\pi}^{\pm}u = \pi^{\pm}u + \alpha_i^{\pm}(t)\psi_{p+1,i}^{\pm}(x),$$

since both $\psi_{p+1,i}^{\pm}(x)$ vanish at the Radau points $x_{i,k}^{\pm}$, $k = 0, 1, \ldots, p$. Since $\hat{\pi}^{-}u(x_{i-1}, t) = u(x_{i-1}, t)$, $\hat{\pi}^{+}u(x_i, t) = u(x_i, t)$, $\psi_{p+1,i}^{-}(x_i) = 0$, and $\psi_{p+1,i}^{+}(x_{i-1}) = 0$, we can use (19) to find

$$\alpha_i^{-}(t) = \frac{u(x_{i-1}, t) - \pi^{-}u(x_{i-1}, t)}{\psi_{p+1,i}^{-}(x_{i-1})}, \quad \alpha_i^{+}(t) = \frac{u(x_i, t) - \pi^{+}u(x_i, t)}{\psi_{p+1,i}^{+}(x_i)}.$$

We note that $\psi_{p+1,i}^{-}(x_{i-1}) \neq 0$ and $\psi_{p+1,i}^{+}(x_i) \neq 0$.

In the next lemma, we recall some properties of $P_h^{\pm}$ and $\pi^{\pm}$ [10], which play important roles in our *a posteriori* error analysis. In particular, we show that the interpolation errors can be divided into significant parts and less significant parts.

Lemma 3.1. *Let u, $q \in H^{p+2}$, $t \in [0, T]$ fixed, and $P_h^{\pm}$ and $\pi^{\pm}$ as defined above. If*

$$(20) \qquad \psi_{p+1,i}^{-}(x) = \prod_{j=0}^{p}(x - x_{i,j}^{-}), \quad \psi_{p+1,i}^{+}(x) = \prod_{j=0}^{p}(x - x_{i,j}^{+}),$$

then the interpolation errors can be split as:

$$(21a) \quad u - \pi^{-}u = \phi_i^{-} + \gamma_i^{-}, \quad \phi_i^{-} = \alpha_i^{-}(t)\psi_{p+1,i}^{-}(x), \quad \gamma_i^{-} = u - \hat{\pi}^{-}u, \quad on\ I_i,$$

$$(21b) \quad q - \pi^{+}q = \phi_i^{+} + \gamma_i^{+}, \quad \phi_i^{+} = \alpha_i^{+}(t)\psi_{p+1,i}^{+}(x), \quad \gamma_i^{+} = q - \hat{\pi}^{+}q, \quad on\ I_i,$$

where $\alpha_i^{-}(t)$ and $\alpha_i^{+}(t)$ are the coefficients of x^{p+1} in the $(p+1)$-degree polynomials $\hat{\pi}^{-}u$ and $\hat{\pi}^{+}q$, respectively, and

$(21c)$
$$\left\|\phi_i^{-}\right\|_{k,I_i} \leq Ch_i^{p+1-k}\left\|u\right\|_{p+1,I_i}, \quad \left\|\phi_i^{+}\right\|_{k,I_i} \leq Ch_i^{p+1-k}\left\|q\right\|_{p+1,I_i}, \quad 0 \leq k \leq p,$$

$(21d)$
$$\left\|\gamma_i^{-}\right\|_{k,I_i} \leq Ch_i^{p+2-k}\left\|u\right\|_{p+2,I_i}, \quad \left\|\gamma_i^{+}\right\|_{k,I_i} \leq Ch_i^{p+2-k}\left\|q\right\|_{p+2,I_i}, 0 \leq k \leq p+1.$$

Moreover,

(22) $\left\|\pi^- u - P_h^- u\right\|_{I_i} \leq Ch_i^{p+2} \left\|u\right\|_{p+2,I_i}, \quad \left\|\pi^+ q - P_h^+ q\right\|_{I_i} \leq Ch_i^{p+2} \left\|q\right\|_{p+2,I_i}.$

Proof. The proof of this lemma can be found in [10], more precisely in its Lemma 3.2. □

Now, we are ready to prove our main superconvergence results. In particular, we show that the significant parts of the discretization errors for the LDG solution and its derivative are proportional to $(p+1)$-degree right and left Radau polynomials, respectively.

Theorem 3. *Under the assumptions of Theorem 1, there exists a constant C such that*

(23) $$\left\|u_h - \pi^- u\right\| \leq Ch^{p+2}, \qquad \left\|q_h - \pi^+ q\right\| \leq Ch^{p+2}.$$

Moreover, the actual errors on I_i can be split as

(24a) $e_u(x,t) = \alpha_i^-(t)\psi_{p+1,i}^-(x) + \omega_i^-(x,t), \quad e_q(x,t) = \alpha_i^+(t)\psi_{p+1,i}^+(x) + \omega_i^+(x,t),$

where

(24b) $$\omega_i^- = \gamma_i^- + \pi^- u - u_h, \quad \omega_i^+ = \gamma_i^+ + \pi^+ q - q_h,$$

and $\forall\, t \in [0,T]$,

(24c) $$\sum_{i=1}^N \left\|\partial_x^k \omega_i^-\right\|_{I_i}^2 \leq Ch^{2(p-k)+4}, \quad \sum_{i=1}^N \left\|\partial_x^k \omega_i^+\right\|_{I_i}^2 \leq Ch^{2(p-k)+4}, \quad k=0,1.$$

Proof. Adding and subtracting $P_h^- u$ to $u_h - \pi^- u$ and $P_h^+ q$ to $q_h - \pi^+ q$, we write

$$u_h - \pi^- u = -\bar{e}_u + P_h^- u - \pi^- u, \quad q_h - \pi^+ q = -\bar{e}_q + P_h^+ q - \pi^+ q.$$

Taking the L^2-norm and applying the triangle inequality, we get

$$\left\|u_h - \pi^- u\right\| \leq \left\|\bar{e}_u\right\| + \left\|P_h^- u - \pi^- u\right\|, \quad \left\|q_h - \pi^+ q\right\| \leq \left\|\bar{e}_q\right\| + \left\|P_h^+ q - \pi^+ q\right\|.$$

Using the estimates (13), and (22) we establish (23).

Adding and subtracting $\pi^- u$ to e_u and $\pi^+ q$ to e_q, we get

$$e_u = u - \pi^- u + \pi^- u - u_h, \quad e_q = q - \pi^+ q + \pi^+ q - q_h.$$

Furthermore, one can split the interpolation errors $u - \pi^- u$ and $q - \pi^+ q$ on I_i as in (21a) and (21b) to obtain

(25a) $e_u = \phi_i^- + \gamma_i^- + \pi^- u - u_h = \phi_i^- + \omega_i^-, \qquad e_q = \phi_i^+ + \gamma_i^+ + \pi^+ q - q_h = \phi_i^+ + \omega_i^+,$

where

(25b) $$\omega_i^- = \gamma_i^- + \pi^- u - u_h, \qquad \omega_i^+ = \gamma_i^+ + \pi^+ q - q_h.$$

Next, we use the Cauchy-Schwarz inequality and the inequality $|ab| \leq \frac{1}{2}(a^2 + b^2)$ to write

$$
\begin{aligned}
\left\|\omega_i^-\right\|_{I_i}^2 &= \int_{I_i} \left(\gamma_i^- + \pi^- u - u_h\right)^2 dx \\
&= \left\|\gamma_i^-\right\|_{I_i}^2 + 2\int_{I_i} \gamma_i^- \left(\pi^- u - u_h\right) dx + \left\|\pi^- u - u_h\right\|_{I_i}^2 \\
&\leq 2\left(\left\|\gamma_i^-\right\|_{I_i}^2 + \left\|\pi^- u - u_h\right\|_{I_i}^2\right),
\end{aligned}
$$

$$\left\|\omega_i^+\right\|_{I_i}^2 = \int_{I_i} \left(\gamma_i^+ + \pi^+ q - q_h\right)^2 dx$$

$$= \left\|\gamma_i^+\right\|_{I_i}^2 + 2\int_{I_i} \gamma_i^+ \left(\pi^+ q - q_h\right) dx + \left\|\pi^+ q - q_h\right\|_{I_i}^2$$

$$\leq 2\left(\left\|\gamma_i^+\right\|_{I_i}^2 + \left\|\pi^+ q - q_h\right\|_{I_i}^2\right).$$

Summing over all elements and applying (21d), and (23) yields

$$\sum_{i=1}^N \left\|\omega_i^-\right\|_{I_i}^2 \leq Ch^{2p+4} + Ch^{2p+4}, \qquad \sum_{i=1}^N \left\|\omega_i^+\right\|_{I_i}^2 \leq Ch^{2p+4} + C_2 h^{2p+4},$$

which complete the proof of (24c) for $k = 0$.

In order to prove the estimates (24c) for $k = 1$, we use the Cauchy-Schwarz inequality and the inequality $|ab| \leq \frac{1}{2}(a^2 + b^2)$ to get

$$\left\|(\omega_i^-)_x\right\|_{I_i}^2 = \int_{I_i} \left(\left(\gamma_i^- + \pi^- u - u_h\right)_x\right)^2 dx \leq 2\left(\left\|(\gamma_i^-)_x\right\|_{I_i}^2 + \left\|(\pi^- u - u_h)_x\right\|_{I_i}^2\right),$$

$$\left\|(\omega_i^+)_x\right\|_{I_i}^2 = \int_{I_i} \left(\left(\gamma_i^+ + \pi^+ q - q_h\right)_x\right)^2 dx \leq 2\left(\left\|(\gamma_i^+)_x\right\|_{I_i}^2 + \left\|(\pi^+ q - q_h)_x\right\|_{I_i}^2\right).$$

Using the inverse inequalities $\left\|(\pi^- u - u_h)_x\right\|_{I_i} \leq ch^{-1}\left\|\pi^- u - u_h\right\|_{I_i}$ and $\left\|(\pi^+ q - q_h)_x\right\|_{I_i} \leq ch^{-1}\left\|\pi^+ q - q_h\right\|_{I_i}$, we obtain the estimates

$$\left\|(\omega_i^-)_x\right\|_{I_i}^2 \leq C\left(\left\|(\gamma_i^-)_x\right\|_{I_i}^2 + h^{-2}\left\|\pi^- u - u_h\right\|_{I_i}^2\right),$$

$$\left\|(\omega_i^+)_x\right\|_{I_i}^2 \leq C\left(\left\|(\gamma_i^+)_x\right\|_{I_i}^2 + h^{-2}\left\|\pi^+ q - q_h\right\|_{I_i}^2\right).$$

Summing over all elements and applying (23) and the standard error estimate (21d), we establish (24c) for $k = 1$. $\qquad\square$

4. *A posteriori* error estimation

A posteriori error estimates lie in the heart of every adaptive finite element algorithm for differential equations. They are used to assess the quality of numerical solutions and guide the adaptive enrichment process where elements having high errors are enriched by *h*-refinement and/or *p*-refinement while elements with small errors are *h*- and/or *p*-coarsened. Furthermore, error estimates are used to stop the adaptive refinement process. For an introduction to the subject of *a posteriori* error estimation see the monograph of Ainsworth and Oden [5]. Several *a posteriori* error estimates are known for hyperbolic [21, 22, 31] and diffusive [32, 35] problems.

In this section, we construct simple, efficient, and asymptotically exact *a posteriori* error estimates. We further use the previous superconvergence results to prove that our proposed *a posteriori* LDG error estimates for the solution and its derivative converge in the L^2-norm to the true spatial errors under mesh refinement. Finally, we prove that the global effectivity index converges in the L^2-norm to unity as $h \to 0$.

We first present the weak finite element formulation to compute *a posteriori* error estimates for the wave equation (1). Replacing u by $u_h + e_u$ and q by $q_h + e_q$ in (2), we have

(26a) $(e_q)_x = (u_h)_{tt} - cu_h - (q_h)_x + (e_u)_{tt} - ce_u, \quad x \in I_i,$

(26b) $(e_u)_x = q_h - (u_h)_x + e_q, \quad x \in I_i.$

Multiplying (26a) and (26b) by arbitrary smooth test functions v and w, respectively, and integrating over I_i, we obtain

$$(27a) \qquad \int_{I_i} (e_q)_x v dx = \int_{I_i} \left((u_h)_{tt} - cu_h - (q_h)_x + (e_u)_{tt} - ce_u \right) v dx,$$

$$(27b) \qquad \int_{I_i} (e_u)_x w dx = \int_{I_i} \left(q_h - (u_h)_x + e_q \right) w dx.$$

Substituting (24a) into the left-hand side of (27) and choosing $v = L_{p,i}(x)$ and $w = L_{p,i}(x)$, we obtain
(28a)
$$\alpha_i^+ \int_{I_i} \left(\psi_{p+1,i}^+ \right)' L_{p,i} dx = \int_{I_i} \left((u_h)_{tt} - cu_h - (q_h)_x + (e_u)_{tt} - ce_u - (\omega_i^+)_x \right) L_{p,i} dx,$$

$$(28b) \qquad \alpha_i^- \int_{I_i} \left(\psi_{p+1,i}^- \right)' L_{p,i} dx = \int_{I_i} \left(q_h - (u_h)_x + e_q - (\omega_i^-)_x \right) L_{p,i} dx.$$

Using the definition of $R_{p+1,i}^{\pm}$ (10) and the orthogonality relation (7b), we get

$$\begin{aligned}
\int_{I_i} \left(\psi_{p+1,i}^{\pm} \right)' L_{p,i} dx &= c_p h_i^{p+1} \int_{I_i} \left(R_{p+1,i}^{\pm} \right)' L_{p,i} dx \\
&= c_p h_i^{p+1} \int_{I_i} \left(L_{p+1,i}' \pm L_{p,i}' \right) L_{p,i} dx = c_p h_i^{p+1} \int_{I_i} L_{p+1,i}' L_{p,i} dx,
\end{aligned}$$

since $L_{p,i}'$ is a polynomial of degree $p-1$. Here, c_p is a constant given by $c_p = \frac{((p+1)!)^2}{(2p+2)!}$.

Using a simple integration by parts and the orthogonality relation (7b), we obtain

$$\begin{aligned}
\int_{I_i} \left(\psi_{p+1,i}^{\pm} \right)' L_{p,i} dx &= c_p h_i^{p+1} \left(L_{p+1,i} L_{p,i}(x_i) - L_{p+1,i} L_{p,i}(x_{i-1}) - \int_{I_i} L_{p+1,i} L_{p,i}' dx \right) \\
&= c_p h_i^{p+1} \left(L_{p+1,i} L_{p,i}(x_i) - L_{p+1,i} L_{p,i}(x_{i-1}) \right).
\end{aligned}$$

By the definition of the Legendre polynomial, we have $\tilde{L}_p(1) = 1$ and $\tilde{L}_p(-1) = (-1)^p$. Therefore, the shifted Legendre polynomials on I_i satisfy $L_{p+1,i}(x_i) = L_{p,i}(x_i) = 1$, $L_{p,i}(x_{i-1}) = (-1)^p$, and $L_{p+1,i}(x_{i-1}) = (-1)^{p+1}$. Thus,

$$(29) \quad \int_{I_i} \left(\psi_{p+1,i}^{\pm} \right)' L_{p,i} dx = c_p h_i^{p+1} \left((1)(1) - (-1)^{p+1}(-1)^p \right) = 2c_p h_i^{p+1}.$$

Substituting (29) into (28) and solving for $\alpha_i^{\pm}$, we obtain

$$(30a) \quad \alpha_i^+ = \frac{1}{2c_p h_i^{p+1}} \int_{I_i} \left((u_h)_{tt} - cu_h - (q_h)_x + (e_u)_{tt} - ce_u - (\omega_i^+)_x \right) L_{p,i} dx,$$

$$(30b) \quad \alpha_i^- = \frac{1}{2c_p h_i^{p+1}} \int_{I_i} \left(q_h - (u_h)_x + e_q - (\omega_i^-)_x \right) L_{p,i} dx.$$

Our error estimate procedure consists of approximating the true errors on each element I_i by the leading terms as

$$(31) \qquad e_u \approx E_u = a_i^-(t) \psi_{p+1,i}^-(x), \quad e_q \approx E_q = a_i^+(t) \psi_{p+1,i}^+(x), \ x \in I_i,$$

where the coefficients of the leading terms of the errors, $a_i^{\pm}$, are obtained from the coefficients $\alpha_i^{\pm}$ defined in (30) by neglecting the terms $\omega_i^{\pm}$, e_u, e_q, and $(e_u)_{tt}$, i.e.,

$$a_i^+ = \frac{1}{2c_p h_i^{p+1}} \int_{I_i} ((u_h)_{tt} - cu_h - (q_h)_x) L_{p,i} dx,$$

$$a_i^- = \frac{1}{2c_p h_i^{p+1}} \int_{I_i} (q_h - (u_h)_x) L_{p,i} dx.$$

We note that E_u and E_q are computable quantities since they only depend on the numerical solutions u_h and q_h. Thus, our LDG error estimates are computationally simple and are obtained by solving a local steady problems with no boundary conditions on each element.

Next, we will show that the error estimates E_u and E_q converge to the true errors e_u and e_q, respectively, in the L^2-norm as $h \to 0$. Furthermore, we will prove the convergence to unity of the global effectivity indices $\Theta_u(t)$ and $\Theta_q(t)$ under mesh refinement.

Before stating our main result we state and prove the following preliminary results.

Theorem 4. *Suppose that (u, q) and (u_h, q_h), respectively, are solutions of (2) and (3). If $\alpha_i^{\pm}$ and $a_i^{\pm}$ are given in (30) and (32) then there exists a constant C such that, at any fixed $t \in [0, T]$,*
(32)
$$\sum_{i=1}^{N} \left(a_i^+ - \alpha_i^+\right)^2 \left\|\psi_{p+1,i}^+\right\|_{I_i}^2 \leq Ch^{2p+4}, \quad \sum_{i=1}^{N} \left(a_i^- - \alpha_i^-\right)^2 \left\|\psi_{p+1,i}^-\right\|_{I_i}^2 \leq Ch^{2p+4}.$$

Proof. Subtracting (32) from (30) and applying the triangle inequality, we get

$$\begin{aligned}
\left|a_i^- - \alpha_i^-\right| &= \frac{1}{2c_p h_i^{p+1}} \left|\int_{I_i} \left(-e_q + (\omega_i^-)_x\right) L_{p,i} dx\right| \\
&\leq \frac{1}{2c_p h_i^{p+1}} \int_{I_i} \left(|e_q| + |(\omega_i^-)_x|\right) |L_{p,i}| dx, \\
\left|a_i^+ - \alpha_i^+\right| &= \frac{1}{2c_p h_i^{p+1}} \left|\int_{I_i} \left(-(e_u)_{tt} + ce_u + (\omega_i^+)_x\right) L_{p,i} dx\right| \\
&\leq \frac{1}{2c_p h_i^{p+1}} \int_{I_i} \left(|(e_u)_{tt}| + |c||e_u| + |(\omega_i^+)_x|\right) |L_{p,i}| dx.
\end{aligned}$$

Using the inequality $\left(\sum_{i=1}^{n} |b_i|\right)^2 \leq n \sum_{i=1}^{n} b_i^2$, which can be easily obtained by applying Young's inequality $2|ab| \leq a^2 + b^2$, with $n = 2$ and $n = 3$ yields

$$\begin{aligned}
(a_i^- - \alpha_i^-)^2 &\leq \frac{1}{2c_p^2 h_i^{2p+2}} \left[\left(\int_{I_i} |e_q||L_{p,i}| dx\right)^2 + \left(\int_{I_i} |(\omega_i^-)_x||L_{p,i}| dx\right)^2\right], \\
(a_i^+ - \alpha_i^+)^2 &\leq \frac{3}{4c_p^2 h_i^{2p+2}} \left[\left(\int_{I_i} |(e_u)_{tt}||L_{p,i}| dx\right)^2 + c^2 \left(\int_{I_i} |e_u||L_{p,i}| dx\right)^2\right. \\
&\qquad\qquad\qquad \left. + \left(\int_{I_i} |(\omega_i^+)_x||L_{p,i}| dx\right)^2\right].
\end{aligned}$$

Applying the Cauchy-Schwarz inequality, we get

$$(33a) \quad (a_i^- - \alpha_i^-)^2 \leq \frac{\|L_{p,i}\|_{I_i}^2}{2c_p^2 h_i^{2p+2}} \left[\|e_q\|_{I_i}^2 + \|(\omega_i^-)_x\|_{I_i}^2\right],$$

$$(33b) \quad (a_i^+ - \alpha_i^+)^2 \leq \frac{3\|L_{p,i}\|_{I_i}^2}{4c_p^2 h_i^{2p+2}} \left[\left(\|(e_u)_{tt}\|_{I_i}^2 + c^2\|e_u\|_{I_i}^2 + \|(\omega_i^+)_x\|_{I_i}^2\right)\right].$$

Using the mapping (9) and the orthogonality relation (7b), we have

$$(34) \qquad \|L_{p,i}\|_{I_i}^2 = \int_{I_i} L_{p,i}^2(t)dt = \frac{h_i}{2}\int_{-1}^{1}\tilde{L}_p^2(\xi)d\xi = \frac{h_i}{2}\frac{2}{2p+1} = \frac{h_i}{2p+1} \leq h_i.$$

Applying (34) and (33) gives

$$(35a) \quad (a_i^- - \alpha_i^-)^2 \leq \frac{1}{2c_p^2 h_i^{2p+1}} \left[\|e_q\|_{I_i}^2 + \|(\omega_i^-)_x\|_{I_i}^2\right],$$

$$(35b) \quad (a_i^+ - \alpha_i^+)^2 \leq \frac{3}{4c_p^2 h_i^{2p+1}} \left[\left(\|(e_u)_{tt}\|_{I_i}^2 + c^2\|e_u\|_{I_i}^2 + \|(\omega_i^+)_x\|_{I_i}^2\right)\right].$$

Multiplying (35a) by $\|\psi_{p+1,i}^-\|_{I_i}^2$ and (35b) by $\|\psi_{p+1,i}^+\|_{I_i}^2$ and using (11) yields

$$(a_i^- - \alpha_i^-)^2 \|\psi_{p+1,i}^-\|_{I_i}^2 \leq 2C_p h_i^2 \left[\|e_q\|_{I_i}^2 + \|(\omega_i^-)_x\|_{I_i}^2\right],$$

$$(a_i^+ - \alpha_i^+)^2 \|\psi_{p+1,i}^+\|_{I_i}^2 \leq 3C_p h_i^2 \left[\left(\|(e_u)_{tt}\|_{I_i}^2 + c^2\|e_u\|_{I_i}^2 + \|(\omega_i^+)_x\|_{I_i}^2\right)\right],$$

where $C_p = \frac{1}{4c_p^2}\frac{2(2p+2)}{(2p+1)(2p+3)}c_p^2 = \frac{(p+1)}{(2p+1)(2p+3)}$.

Finally, summing over all elements and using the fact that $h = \max\limits_{1 \leq i \leq N} h_i$, we arrive at

$$\sum_{i=1}^{N}(a_i^- - \alpha_i^-)^2 \|\psi_{p+1,i}^-\|_{I_i}^2 \leq 2C_p h^2 \left[\|e_q\|^2 + \sum_{i=1}^{N}\|(\omega_i^-)_x\|_{I_i}^2\right],$$

$$\sum_{i=1}^{N}(a_i^+ - \alpha_i^+)^2 \|\psi_{p+1,i}^+\|_{I_i}^2 \leq 3C_p h^2 \left[\|(e_u)_{tt}\|^2 + c^2\|e_u\|^2 + \sum_{i=1}^{N}\|(\omega_i^+)_x\|_{I_i}^2\right].$$

Applying the estimates (15), (16), (17), and (24c), we establish (32). $\square$

The main results of this section are stated in the following theorem. In particular, we prove optimal convergence rates in the L^2-norm for the *a posteriori* error estimates (31) and for the global effectivity indices.

Theorem 5. *Suppose that the assumptions of Theorem 1 are satisfied. If $\alpha_i^\pm$ and $a_i^\pm$ are given by (30) and (32), respectively, and*

$$E_u(x,t) = a_i^-(t)\psi_{p+1,i}^-(x), \qquad E_q(x,t) = a_i^+(t)\psi_{p+1,i}^+(x), \ x \in I_i,$$

then there exists a positive constant C independent of h such that

$$(37) \qquad \|e_u - E_u\| \leq Ch^{p+2}, \quad \|e_q - E_q\| \leq Ch^{p+2}.$$

Consequently, there exist positive constants C_1 and C_2 independent of h such that

$$(38) \qquad \left|\, \|e_u\| - \|E_u\|\,\right| \leq C_1 h^{p+2}, \quad \left|\, \|e_q\| - \|E_q\|\,\right| \leq C_2 h^{p+2}.$$

Finally, at a fixed time t, the global effectivity indices in the L^2 converge to unity at $\mathcal{O}(h)$ rate i.e.,

$$(39) \qquad \Theta_u(t) = \frac{\|E_u\|}{\|e_u\|} = 1 + \mathcal{O}(h), \qquad \Theta_q(t) = \frac{\|E_q\|}{\|e_q\|} = 1 + \mathcal{O}(h).$$

Proof. First, we will prove (37). Since $e_u = \alpha_i^- \psi_{p+1,i}^- + \omega_i^-$, $e_q = \alpha_i^+ \psi_{p+1,i}^+ + \omega_i^+$, $E_u = a_i^- \psi_{p+1,i}^-$, and $E_q = a_i^+ \psi_{p+1,i}^+$ on I_i, we have

$$\|e_u - E_u\|_{I_i}^2 = \|(\alpha_i^- - a_i^-)\psi_{p+1,i}^- + \omega_i^-\|_{I_i}^2 \le 2(\alpha_i^- - a_i^-)^2 \|\psi_{p+1,i}^-\|_{I_i}^2 + 2\|\omega_i^-\|_{I_i}^2,$$

$$\|e_q - E_q\|_{I_i}^2 = \|(\alpha_i^+ - a_i^+)\psi_{p+1,i}^+ + \omega_i^+\|_{I_i}^2 \le 2(\alpha_i^+ - a_i^+)^2 \|\psi_{p+1,i}^+\|_{I_i}^2 + 2\|\omega_i^+\|_{I_i}^2,$$

where we used the inequality $(a+b)^2 \le 2a^2 + 2b^2$. Summing over all elements and applying the estimates (24c) and (32) yields

$$
\begin{aligned}
\|e_u - E_u\|^2 &= \sum_{i=1}^{N} \|e_u - E_u\|_{I_i}^2 \\
&\le 2\sum_{i=1}^{N}(\alpha_i^- - a_i^-)^2 \|\psi_{p+1,i}^-\|_{I_i}^2 + 2\sum_{i=1}^{N}\|\omega_i^-\|_{I_i}^2 \le Ch^{2p+4},
\end{aligned}
$$

$$
\begin{aligned}
\|e_q - E_q\|^2 &= \sum_{i=1}^{N} \|e_q - E_q\|_{I_i}^2 \\
&\le 2\sum_{i=1}^{N}(\alpha_i^+ - a_i^+)^2 \|\psi_{p+1,i}^+\|_{I_i}^2 + 2\sum_{i=1}^{N}\|\omega_i^+\|_{I_i}^2 \le Ch^{2p+4}.
\end{aligned}
$$

Next, we will prove (38). Using the reverse triangle inequality, we have

$$(40) \qquad \big| \|E_u\| - \|e_u\| \big| \le \|E_u - e_u\|, \quad \big| \|E_q\| - \|e_q\| \big| \le \|E_q - e_q\|.$$

Combining (40) and (37) completes the proof of (38).

Finally, the estimate (39) can be deduced from the estimate (37) and the fact that u_h and q_h are $\mathcal{O}(h^{p+2})$ super close to the Gauss-Radau projections $P_h^- u$ and $P_h^+ q$, respectively. $\qquad\square$

An accepted efficiency measure of *a posteriori* error estimates is the effectivity index. In this paper, we use the global effectivity indices $\Theta_u(t) = \frac{\|E_u\|}{\|e_u\|}$ and $\Theta_q(t) = \frac{\|E_q\|}{\|e_q\|}$. Ideally, the global effectivity indices should stay close to one and should converge to one under mesh refinement.

In the previous theorem, we proved that the *a posteriori* error estimates, at a fixed time t, converge to the true spatial errors at $\mathcal{O}(h^{p+2})$ rate. We also proved that the global effectivity index in the L^2-norm converges to unity at $\mathcal{O}(h)$ rate.

Remark 4.1. The estimates in (38) indicate that $\|e_u\| = \|E_u\| + \mathcal{O}(h^{p+2})$ and $\|e_q\| = \|E_q\| + \mathcal{O}(h^{p+2})$ with

$$
\begin{aligned}
\|E_u\|^2 &= \sum_{i=1}^{N} \|E_u\|_{I_i}^2 = \sum_{i=1}^{N}(a_i^-(t))^2 \|\psi_{p+1,i}^-\|_{I_i}^2 \\
&= \frac{(p+1)}{(2p+1)(2p+3)} \sum_{i=1}^{N} h_i \left(\int_{I_i} (q_h - (u_h)_x) L_{p,i} dx \right)^2.
\end{aligned}
$$

$$\begin{aligned} \|E_q\|^2 &= \sum_{i=1}^{N} \|E_q\|_{I_i}^2 = \sum_{i=1}^{N} (a_i^+(t))^2 \left\|\psi_{p+1,i}^+\right\|_{I_i}^2 \\ &= \frac{(p+1)}{(2p+1)(2p+3)} \sum_{i=1}^{N} h_i \left(\int_{I_i} ((u_h)_{tt} - cu_h - (q_h)_x) \, L_{p,i} dx \right)^2, \end{aligned}$$

where we used (11) and (32).

Remark 4.2. The performance of an error estimator is commonly measured by the effectivity index which is the ratio of the estimated error to the actual error. In particular, we say that the error estimator is asymptotically exact if the effectivity index approaches unity as the mesh size goes to zero. We note that (39) indicates that the computable quantity $\|E_u\|$ provides an asymptotically exact *a posteriori* estimator on the actual error $\|e_u\|$.

Remark 4.3. We would like to mention that the computable quantities $u_h + E_u$ and $q_h + E_q$ converge to the exact solutions u and q at $\mathcal{O}(h^{p+2})$ rate. We emphasize that this accuracy enhancement is achieved by adding the error estimates to the approximate solutions only once at the end of the computation *i.e.*, at $t = T$.

5. Numerical examples

In this section, we present several numerical examples to validate the optimal convergence rates in the L^2-norm for the *a posteriori* error estimates (31)-(32). The initial conditions are obtained using (12) with $l = 1$. We also observed similar results when using the projection P_h^- *i.e.*, $u_h(x,0) = P_h^- u(x,0)$ and $(u_h)_t(x,0) = P_h^- u_t(x,0)$. Temporal integration is performed by the ninth order strong-stability preserving (SSP) Runge-Kutta method [30]. The time step is chosen so that temporal errors are small relative to spatial errors. In our experiments, we take $\Delta t = 0.001 h_{min}$ to reduce the time error.

Example 5.1. In this example, we consider the following problem subject to the mixed Dirichlet-Neumann boundary conditions

(41)
$$\begin{cases} u_{tt} - u_{xx} = 0, & x \in [0,5], \quad t \in [0,1], \\ u(x,0) = e^x, & u_t(x,0) = e^x, \quad x \in [0,5], \\ u(0,t) = e^t, & u_x(5,t) = e^{5+t}, \quad t \in [0,1]. \end{cases}$$

The exact solution is given by $u(x,t) = e^{x+t}$. We use the numerical fluxes

$$\hat{u}_h\big|_i = \begin{cases} u(0,t), & i = 0, \\ u_h^-\big|_i, & i = 1,\dots,N, \end{cases}, \quad \hat{q}_h\big|_i = \begin{cases} q_h^+\big|_i, & i = 0,\dots,N-1, \\ u_x(5,t), & i = N. \end{cases}$$

We solve this problem using the LDG method on uniform meshes having $N = 5$, 10, 15, 20, 25, 30, 35, 40 elements and using the space P^p with $p = 1-4$. In Figure 1 we present the errors $\|u_h - \pi^- u\|$ and $\|q_h - \pi^+ q\|$ at time $t = 1$. These results indicate that both errors converge at $\mathcal{O}(h^{p+2})$ rate. Thus, the superconvergence rate proved in this paper is optimal in the exponent of the parameter h. This is in full agreement with the theory.

We apply the error estimation procedure (31)-(32) to compute error estimates for the LDG solution and its derivative. The results shown in Figure 2 indicate that the errors $\|e_u - E_u\| = \mathcal{O}(h^{p+2})$ and $\|e_q - E_q\| = \mathcal{O}(h^{p+2})$ at $t = 1$. We note that

$$\|e_u - E_u\| = \|u - (u_h + E_u)\| = \mathcal{O}(h^{p+2}), \quad \|e_q - E_q\| = \|q - (q_h + E_q)\| = \mathcal{O}(h^{p+2}).$$

As a consequence, the LDG method combined with our *a posteriori* error estimation procedure yields both accurate error estimates and $\mathcal{O}(h^{p+2})$ superconvergent solutions. More precisely, the computable quantities $u_h + E_u$ and $q_h + E_q$, respectively, converge in the L^2-norm to the exact solutions u and q at $\mathcal{O}(h^{p+2})$. We emphasize that this accuracy enhancement is achieved by adding the error estimates E_u and E_q to the approximate solutions u_h and q_h only once at the end of the computation *i.e.*, at $t = T$. This leads to very efficient computations of the post-processed approximations $u_h + E_u$ and $q_h + E_q$. Additionally, it is computationally efficient because our LDG error estimates are obtained by solving a local steady problem with no boundary conditions on each element.

Next, we present the global effectivity indices Θ_u and Θ_q in Table 1. These results suggest that the global effectivity indices converge to unity under h-refinement. The results shown in Figure 3 indicate that the errors $\big| \|e_u\| - \|E_u\| \big|$ and $\big| \|e_q\| - \|E_q\| \big|$ at $t = 1$ are both $\mathcal{O}(h^{p+2})$. Finally, we present the errors $\big| \Theta_u - 1 \big|$ and $\big| \Theta_q - 1 \big|$ in Figure 4. These results indicate that the convergence rate at $t = 1$ for $\big| \Theta_u - 1 \big|$ and $\big| \Theta_q - 1 \big|$ is $\mathcal{O}(h)$ under mesh refinement. This example demonstrates that the convergence rates proved in this paper are optimal.
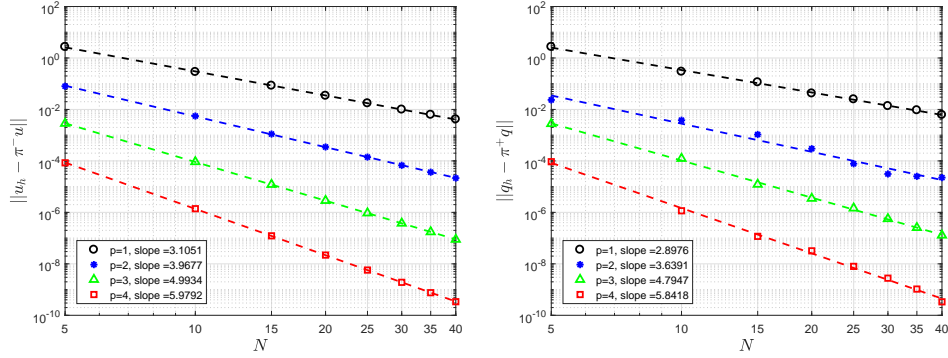

Figure 1: Convergence rates at $t = 1$ for $\|u_h - \pi^- u\|$ (left) and $\|q_h - \pi^+ q\|$ (right) for Example 5.1 on uniform meshes having $N = 5, 10, 15, 20, 25, 30, 35, 40$ elements and using the spaces P^p, $p = 1, 2, 3, 4$. The slopes of the fitting lines are shown on the graph.

TABLE 1. Global effectivity indices Θ_u and Θ_q at $t = 1$ for Example 5.1 on uniform meshes having $N = 5, 10, 15, 20, 25, 30, 35, 40$ elements using P^p, $p = 1, 2, 3, 4$.

| N	$p = 1$		$p = 2$		$p = 3$		$p = 4$	
	Θ_u	Θ_q	Θ_u	Θ_q	Θ_u	Θ_q	Θ_u	Θ_q
5	0.89614	1.0916	0.91813	1.0700	0.93914	1.0686	0.95100	1.0587
10	0.94282	1.0508	0.95870	1.0358	0.96919	1.0373	0.97516	1.0244
15	0.96131	1.0376	0.97247	1.0258	0.97939	1.0185	0.98339	1.0152
20	0.97018	1.0283	0.97928	1.0185	0.98447	1.0152	0.98754	1.0142
25	0.97602	1.0243	0.98338	1.0138	0.98757	1.0140	0.99002	1.0103
30	0.97979	1.0205	0.98616	1.0125	0.98965	1.0095	0.99168	1.0092
35	0.98263	1.0185	0.98816	1.0126	0.99110	1.0086	0.99287	1.0082
40	0.98472	1.0164	0.98964	1.0112	0.99221	1.0080	0.99376	1.0063
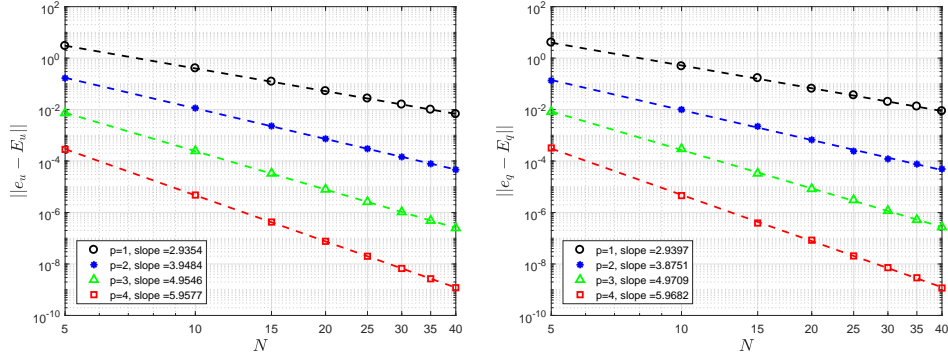
Figure 2: Convergence rates at $t = 1$ for $||e_u - E_u||$ (left) and $||e_q - E_q||$ (right) for Example 5.1 on uniform meshes having $N = 5, 10, 15, 20, 25, 30, 35, 40$ elements and using the spaces P^p, $p = 1, 2, 3, 4$. The slopes of the fitting lines are shown on the graph.
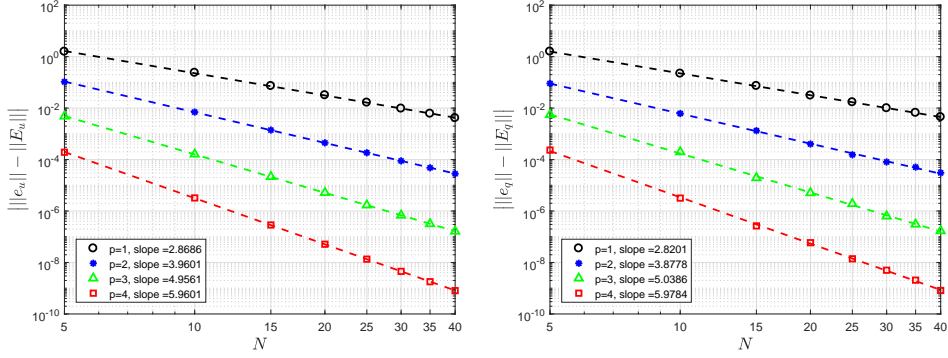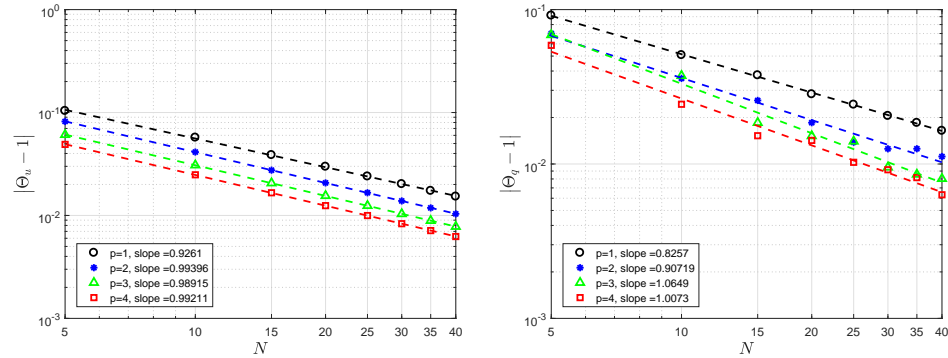

Figure 3: Convergence rates at $t = 1$ for $\left| ||e_u|| - ||E_u|| \right|$ (left) and $\left| ||e_q|| - ||E_q|| \right|$ (right) for Example 5.1 on uniform meshes having $N = 5, 10, 15, 20, 25, 30, 35, 40$ elements and using the spaces P^p, $p = 1, 2, 3, 4$. The slopes of the fitting lines are shown on the graph.

Figure 4: Convergence rates at $t = 1$ for $\left| \Theta_u - 1 \right|$ (left) and $\left| \Theta_q - 1 \right|$ (right) for Example 5.1 on uniform meshes having $N = 5, 10, 20, 40, 80, 160$ elements and using the spaces P^p, $p = 1, 2, 3, 4$. The slopes of the fitting lines are shown on the graph.

Example 5.2. We consider the following wave equation with $\alpha = 0$

$$(42) \qquad \begin{cases} u_{tt} = u_{xx}, & x \in [0, 2\pi], \quad t \in [0, 1], \\ u(x, 0) = e^{\sin(x)}, & u_t(x, 0) = -e^{\sin(x)} \cos(x), \quad x \in [0, 2\pi], \end{cases}$$

subject to the periodic boundary conditions (1c). The exact solution is $u(x, t) = e^{\sin(x-t)}$. We solve this problem using the LDG method on uniform meshes having $N = 5, 10, 20, 40, 80, 160$ elements. We compute the LDG solutions in the spaces P^p, $p = 1, 2, 3, 4$. The L^2 error norms between the LDG solutions (u_h, q_h) and the Radau interpolating polynomials $(\pi^- u, \pi^+ q)$ as well as their order of convergence at $t = 1$ are shown in Figure 5. These results suggest that the LDG solutions u_h and q_h are $\mathcal{O}(h^{p+2})$ super close to $\pi^- u$ and $\pi^+ q$, respectively. This is in full agreement with the theory.

We apply the error estimation procedure (31)-(32) to compute error estimates for the LDG solution and its derivative. The results shown in Figure 6 indicate that the errors $||e_u - E_u||$ and $||e_q - E_q||$ at $t = 1$ are both $\mathcal{O}(h^{p+2})$. This example demonstrates that the convergence rate proved in this paper is optimal. The global effectivity indices Θ_u and Θ_q shown in Table 2 suggest that the global effectivity indices converge to unity under h-refinement. In Figure 7 we present the convergence rates at $t = 1$ for $\big|||e_u|| - ||E_u||\big|$ and $\big|||e_q|| - ||E_q||\big|$. These results indicate that the convergence rate is higher than the theoretical rate established in Theorem 5, which is proved to be of order $p + 2$. Finally, we present the errors $\big|\Theta_u - 1\big|$ and $\big|\Theta_q - 1\big|$ in Figure 8. These results indicate that the convergence rates at $t = 1$ for $\big|\Theta_u - 1\big|$ and $\big|\Theta_q - 1\big|$ are, respectively, $\mathcal{O}(h^{p+2})$ and $\mathcal{O}(h^2)$ under mesh refinement. We remark that the observed numerical convergence rate for $\big|\Theta_u - 1\big|$ is higher than the theoretical rate established in Theorem 5.
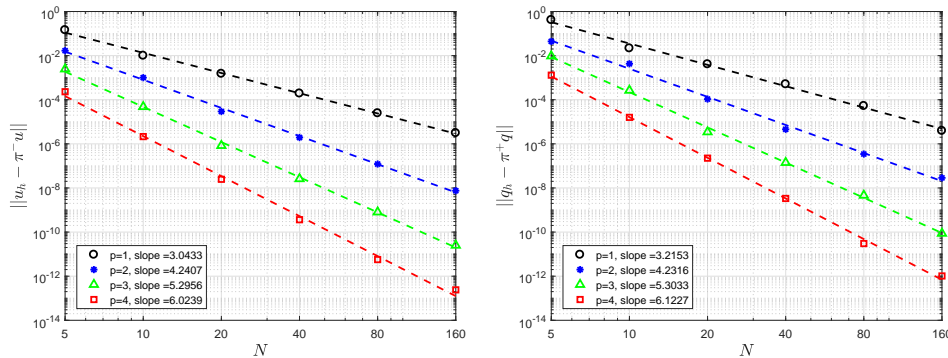

Figure 5: Convergence rates at $t = 1$ for $||u_h - \pi^- u||$ (left) and $||q_h - \pi^+ q||$ (right) for Example 5.2 on uniform meshes having $N = 5, 10, 20, 40, 80, 160$ elements and using the spaces P^p, $p = 1, 2, 3, 4$. The slopes of the fitting lines are shown on the graph.

Example 5.3. We consider the following linear wave equation with $\alpha = -1$

$$(43) \qquad \begin{cases} u_{tt} + u = u_{xx}, & x \in [0, 2\pi], \quad 0 \le t \le 1, \\ u(x, 0) = \sin(x), & u_t(x, 0) = \sqrt{2} \cos(x), \quad x \in [0, 2\pi], \end{cases}$$

subject to the periodic boundary conditions. The exact solution is given by $u(x, t) = \sin(x + \sqrt{2}t)$. We solve this problem using the LDG method on uniform meshes
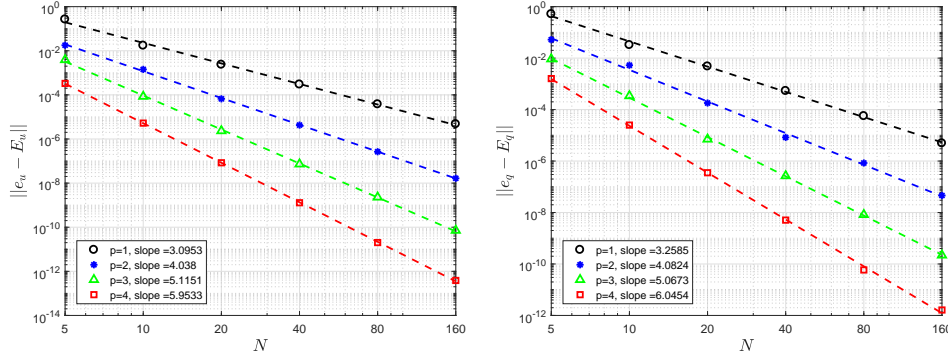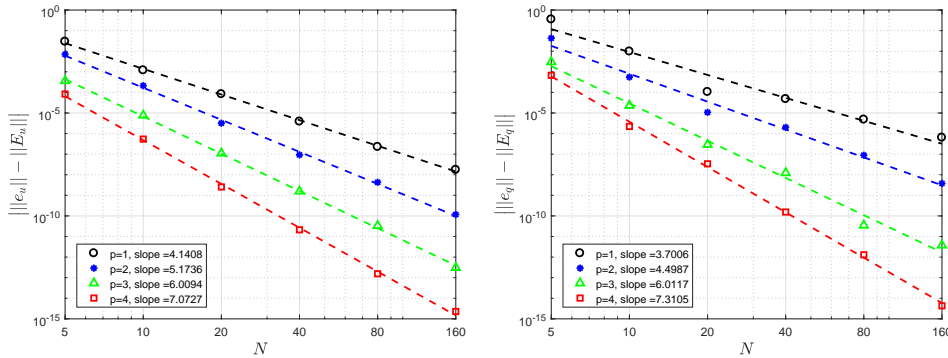
Figure 6: Convergence rates at $t = 1$ for $||e_u - E_u||$ (left) and $||e_q - E_q||$ (right) for Example 5.2 on uniform meshes having $N = 5, 10, 20, 40, 80, 160$ elements and using the spaces P^p, $p = 1, 2, 3, 4$. The slopes of the fitting lines are shown on the graph.

TABLE 2. Global effectivity indices Θ_u and Θ_q at $t = 1$ for Example 5.2 on uniform meshes having $N = 5, 10, 20, 40, 80, 160$ elements using P^p, $p = 1, 2, 3, 4$.

	$p = 1$		$p = 2$		$p = 3$		$p = 4$	
N	Θ_u	Θ_q	Θ_u	Θ_q	Θ_u	Θ_q	Θ_u	Θ_q
5	0.90205	0.48738	0.88247	0.19507	1.09140	0.89771	0.94720	0.75024
10	0.98295	0.91286	0.96499	0.95975	0.98436	0.98205	0.98613	0.97954
20	0.99522	1.00340	0.99566	1.00700	0.99640	0.99621	0.99789	0.99038
40	0.99911	1.00640	0.99900	0.98990	0.99918	1.00250	0.99944	0.99860
80	0.99979	1.00260	0.99963	1.00360	0.99972	1.00010	0.99987	1.00040
160	0.99994	0.99860	0.99992	1.00120	0.99996	0.99980	0.99994	0.99996

Figure 7: Convergence rates at $t = 1$ for $\big|\,||e_u|| - ||E_u||\,\big|$ (left) and $\big|\,||e_q|| - ||E_q||\,\big|$ (right) for Example 5.2 on uniform meshes having $N = 5, 10, 20, 40, 80, 160$ elements and using the spaces P^p, $p = 1, 2, 3, 4$. The slopes of the fitting lines are shown on the graph.

having $N = 5, 10, 20, 40, 80$ elements and using the spaces P^p with $p = 1, 2, 3$, and 4. The L^2 error norms between the LDG solutions (u_h, q_h) and the Radau interpolating polynomials $(\pi^- u, \pi^+ q)$ as well as their order of convergence at $t = 1$ are shown in Figure 9. These results suggest that the LDG solutions u_h and q_h are $\mathcal{O}(h^{p+2})$
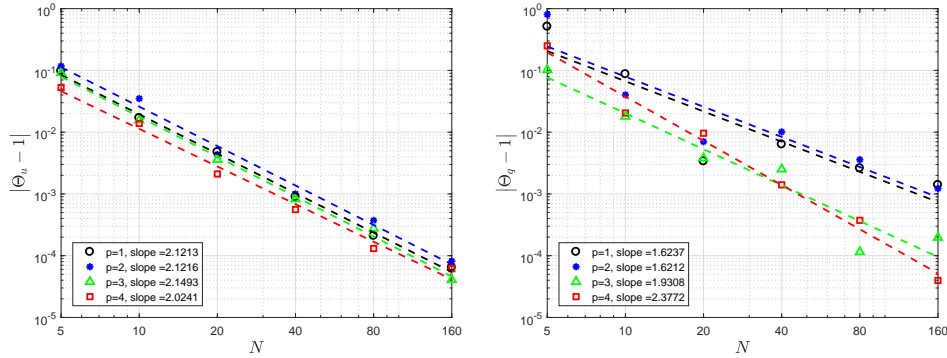
Figure 8: Convergence rates at $t = 1$ for $|\Theta_u - 1|$ (left) and $|\Theta_q - 1|$ (right) for Example 5.2 on uniform meshes having $N = 5, 10, 20, 40, 80, 160$ elements and using the spaces P^p, $p = 1, 2, 3, 4$. The slopes of the fitting lines are shown on the graph.

super close to $\pi^- u$ and $\pi^+ q$, respectively. We apply the error estimation procedure (31)-(32) to compute error estimates for the LDG solution and its derivative. In Figure 10 we present the global errors $||e_u - E_u||$ and $||e_q - E_q||$ at $t = 1$. These results indicate that $||e_u - E_u|| = \mathcal{O}(h^{p+2})$ and $||e_q - E_q|| = \mathcal{O}(h^{p+2})$. This is in full agreement with the theory. Next, we present the global effectivity indices Θ_u and Θ_q in Table 3. We observe that the global effectivity indices converge to unity under h-refinement. The results shown in Figure 11 indicate that the convergence rates at $t = 1$ for $|||e_u|| - ||E_u|||$ and $|\Theta_u - 1|$ are, respectively, $\mathcal{O}(h^{p+2})$ and $\mathcal{O}(h^2)$ under mesh refinement. We remark that the observed numerical convergence rate for $|\Theta_u - 1|$ is higher than the theoretical rate established in Theorem 5.
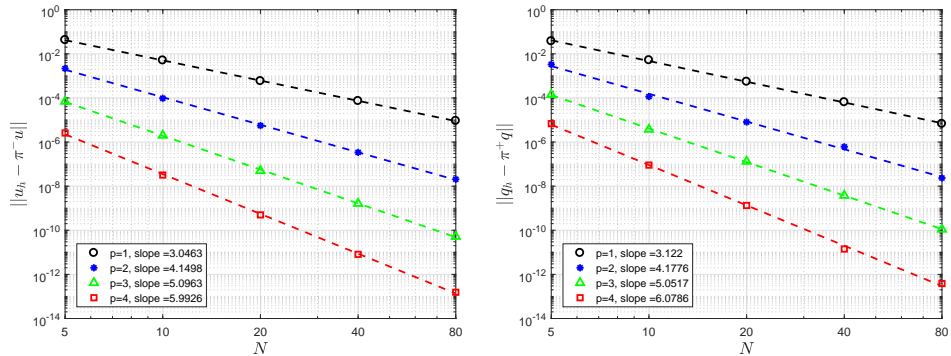

Figure 9: Convergence rates at $t = 1$ for $||u_h - \pi^- u||$ (left) and $||q_h - \pi^+ q||$ (right) for Example 5.3 on uniform meshes having $N = 5, 10, 20, 40, 80$ elements and using the spaces P^p, $p = 1, 2, 3, 4$. The slopes of the fitting lines are shown on the graph.

6. Concluding remarks

In this paper, we studied the global convergence of the implicit residual-based *a posteriori* LDG error estimates of the LDG method for the linear second-order wave equation in one space dimension. We used recent optimal superconvergence results to prove that the LDG solution and its spatial derivative, respectively, converge in the L^2-norm to $(p+1)$-degree right and left Radau interpolating polynomials under
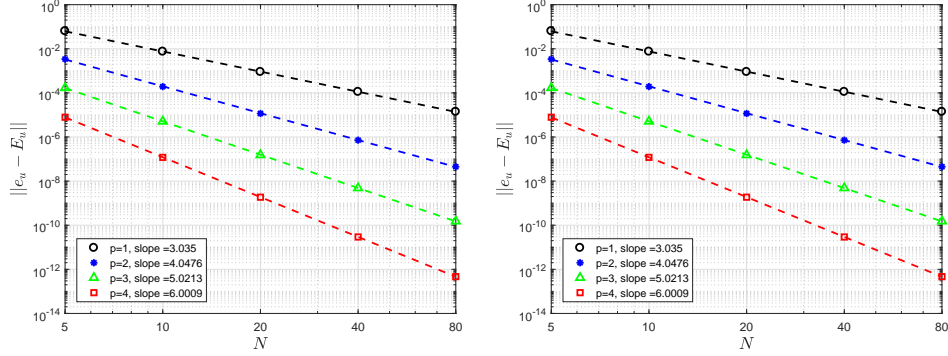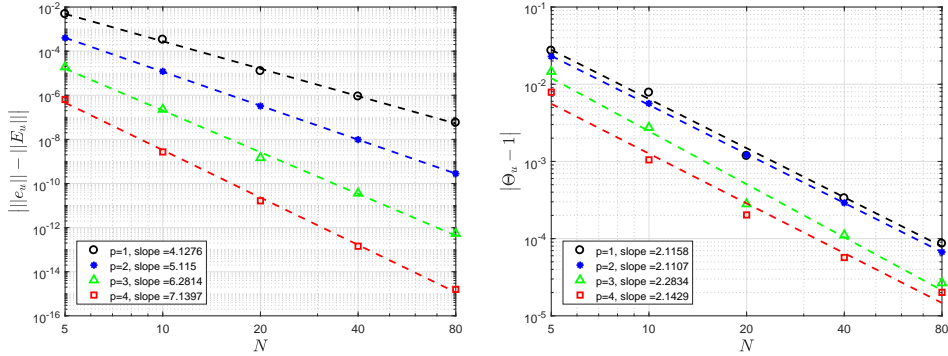
Figure 10: Convergence rates at $t = 1$ for $||e_u - E_u||$ (left) and $||e_q - E_q||$ (right) for Example 5.3 on uniform meshes having $N = 5, 10, 20, 40, 80$ elements and using the spaces P^p, $p = 1, 2, 3, 4$. The slopes of the fitting lines are shown on the graph.

TABLE 3. Global effectivity indices Θ_u and Θ_q at $t = 1$ for Example 5.3 on uniform meshes having $N = 5, 10, 20, 40, 80$ elements using P^p, $p = 1, 2, 3, 4$.

| | $p = 1$ | | $p = 2$ | | $p = 3$ | | $p = 4$ | |
N	Θ_u	Θ_q	Θ_u	Θ_q	Θ_u	Θ_q	Θ_u	Θ_q
5	0.97269	0.92902	0.97712	1.01130	0.98539	0.99409	0.99211	0.97793
10	0.99219	1.01960	0.99436	0.97160	0.99725	0.99849	0.99895	0.98477
20	0.99882	0.97629	0.99879	0.99822	0.99972	1.01140	0.99980	0.99520
40	0.99967	0.99029	0.99971	1.00620	0.99989	0.99848	0.99994	1.00080
80	0.99991	0.99708	0.99993	0.99667	0.99997	1.00190	0.99998	1.00160

Figure 11: Convergence rates at $t = 1$ for $\left| ||e_u|| - ||E_u|| \right|$ (left) and $\left| \Theta_u - 1 \right|$ (right) for Example 5.3 on uniform meshes having $N = 5, 10, 20, 40, 80$ elements and using the spaces P^p, $p = 1, 2, 3, 4$. The slopes of the fitting lines are shown on the graph.

mesh refinement. The order of convergence is proved to be $p + 2$, when piecewise polynomials of degree at most p are used. We used these results to show that the leading error terms on each element for the solution and its derivative are proportional to $(p+1)$-degree right and left Radau polynomials. Furthermore, we obtained optimal convergence rate in the L^2-norm for the *a posteriori* error estimates. The order of convergence is proved to be $p + 2$. As a consequence, we proved that

the LDG method combined with the *a posteriori* error estimation procedure yields both accurate error estimates and $\mathcal{O}(h^{p+2})$ superconvergent solutions. Finally, we proved that the global effectivity indices, for both the solution and its derivative, in the L^2-norm converge to unity at $\mathcal{O}(h)$. Our results are valid for arbitrary regular meshes and schemes with $p \geq 1$. These results improve upon our previously published work [12] in which the order of convergence in the L^2-norm for the *a posteriori* error estimates and the global effectivity index are proved to be $p + 3/2$ and $1/2$, respectively. We are currently investigating the superconvergence properties and the asymptotic exactness of implicit *a posteriori* error estimates for LDG methods applied to nonlinear problems on rectangular and triangular meshes. Our future work will also focus on using these *a posteriori* error estimates to construct efficient adaptive high-order LDG methods.

Acknowledgments

References

[1] M. Abramowitz, I. A. Stegun, Handbook of Mathematical Functions, Dover, New York, 1965.

[2] S. Adjerid, M. Baccouch, A superconvergent local discontinuous Galerkin method for elliptic problems, Journal of Scientific Computing 52 (2012) 113–152.

[3] S. Adjerid, D. Issaev, Superconvergence of the local discontinuous Galerkin method applied to diffusion problems, in: K. Bathe (ed.), Proceedings of the Third MIT Conference on Computational Fluid and Solid Mechanics, vol. 3, Elsevier, 2005.

[4] S. Adjerid, A. Klauser, Superconvergence of discontinuous finite element solutions for transient convection-diffusion problems, Journal of Scientific Computing 22 (2005) 5–24.

[5] M. Ainsworth, J. T. Oden, *A posteriori* Error Estimation in Finite Element Analysis, John Wiley, New York, 2000.

[6] M. Baccouch, A local discontinuous Galerkin method for the second-order wave equation, Computer Methods in Applied Mechanics and Engineering 209–212 (2012) 129–143.

[7] M. Baccouch, Asymptotically exact *a posteriori* LDG error estimates for one-dimensional transient convection-diffusion problems, Applied Mathematics and Computation 226 (2014) 455 – 483.

[8] M. Baccouch, The local discontinuous Galerkin method for the fourth-order Euler-Bernoulli partial differential equation in one space dimension. Part I: Superconvergence error analysis, Journal of Scientific Computing 59 (2014) 795–840.

[9] M. Baccouch, Superconvergence and *a posteriori* error estimates for the LDG method for convection-diffusion problems in one space dimension, Computers & Mathematics with Applications 67 (2014) 1130–1153.

[10] M. Baccouch, Superconvergence of the local discontinuous Galerkin method applied to the one-dimensional second-order wave equation, Numerical methods for partial differential equations 30 (2014) 862–901.

[11] M. Baccouch, A superconvergent local discontinuous Galerkin method for the second-order wave equation on cartesian grids, Computers and Mathematics with Applications 68 (2014) 1250–1278.

[12] M. Baccouch, Asymptotically exact *a posteriori* local discontinuous Galerkin error estimates for the one-dimensional second-order wave equation, Numerical methods for partial differential equations 31 (2015) 1461–1491.

[13] W. Cao, D. Li, Z. Zhang, Optimal superconvergence of energy conserving local discontinuous Galerkin methods for wave equations, Communications in Computational Physics 21 (1) (2017) 211–236.

[14] W. Cao, Z. Zhang, Superconvergence of local discontinuous Galerkin methods for one-dimensional linear parabolic equations, Mathematics of Computation 85 (297) (2016) 63–84.

[15] P. Castillo, A superconvergence result for discontinuous Galerkin methods applied to elliptic problems, Computer Methods in Applied Mechanics and Engineering 192 (2003) 4675–4685.

[16] P. Castillo, A review of the Local Discontinuous Galerkin (LDG) method applied to elliptic problems, Applied Numerical Mathematics 56 (2006) 1307–1313.

[17] P. Castillo, B. Cockburn, D. Schötzau, C. Schwab, Optimal a priori error estimates for the *hp*-version of the local discontinuous Galerkin method for convection-diffusion problems, Mathematic of Computation 71 (2002) 455–478.

[18] F. Celiker, B. Cockburn, Superconvergence of the numerical traces for discontinuous Galerkin and hybridized methods for convection-diffusion problems in one space dimension, Mathematics of Computation 76 (2007) 67–96.

[19] Y. Cheng, C.-W. Shu, Superconvergence of discontinuous Galerkin and local discontinuous Galerkin schemes for linear hyperbolic and convection-diffusion equations in one space dimension, SIAM Journal on Numerical Analysis 47 (2010) 4044–4072.

[20] P. G. Ciarlet, The finite element method for elliptic problems, North-Holland Pub. Co., Amsterdam-New York-Oxford, 1978.

[21] B. Cockburn, A simple introduction to error estimation for nonlinear hyperbolic conservation laws, in: Proceedings of the 1998 EPSRC Summer School in Numerical Analysis, SSCM, volume 26 of the Graduate Student's Guide for Numerical Analysis, pages 1-46, Springer, Berlin, 1999.

[22] B. Cockburn, P. A. Gremaud, Error estimates for finite element methods for nonlinear conservation laws, SIAM Journal on Numerical Analysis 33 (1996) 522–554.

[23] B. Cockburn, G. Kanschat, D. Schötzau, A locally conservative LDG method for the incompressible Navier-Stokes equations, Mathematics of compuatation 74 (2004) 1067–1095.

[24] B. Cockburn, G. Kanschat, D. Schötzau, The local discontinuous Galerkin method for linearized incompressible fluid flow: a review, Computers & Fluids 34 (4-5) (2005) 491 – 506.

[25] B. Cockburn, G. E. Karniadakis, C. W. Shu, Discontinuous Galerkin Methods Theory, Computation and Applications, Lecture Notes in Computational Science and Engineering, vol. 11, Springer, Berlin, 2000.

[26] B. Cockburn, C. W. Shu, TVB Runge-Kutta local projection discontinuous Galerkin methods for scalar conservation laws II: General framework, Mathematics of Computation 52 (1989) 411–435.

[27] B. Cockburn, C. W. Shu, The local discontinuous Galerkin method for time-dependent convection-diffusion systems, SIAM Journal on Numerical Analysis 35 (1998) 2440–2463.

[28] K. D. Devine, J. E. Flaherty, Parallel adaptive *hp*-refinement techniques for conservation laws, Computer Methods in Applied Mechanics and Engineering 20 (1996) 367–386.

[29] J. E. Flaherty, R. Loy, M. S. Shephard, B. K. Szymanski, J. D. Teresco, L. H. Ziantz, Adaptive local refinement with octree load-balancing for the parallel solution of three-dimensional conservation laws, Journal of Parallel and Distributed Computing 47 (1997) 139–152.

[30] S. Gottlieb, C.-W. Shu, E. Tadmor, Strong stability-preserving high-order time discretization methods, SIAM Review 43 (1) (2001) 89–112.

[31] R. Hartmann, P. Houston, Adaptive discontinuous Galerkin finite element methods for nonlinear hyperbolic conservations laws, SIAM Journal on Scientific Computing 24 (2002) 979–1004.

[32] P. Houston, D. Schötzau, T. Wihler, Energy norm *a posteriori* error estimation of *hp*-adaptive discontinuous Galerkin methods for elliptic problems, Mathematical Models and Methods in Applied Sciences 17 (2007) 33–62.

[33] X. Meng, C.-W. Shu, Q. Zhang, B. Wu, Superconvergence of discontinuous Galerkin methods for scalar nonlinear conservation laws in one space dimension, SIAM Journal on Numerical Analysis 50 (5) (2012) 2336–2356.

[34] W. H. Reed, T. R. Hill, Triangular mesh methods for the neutron transport equation, Tech. Rep. LA-UR-73-479, Los Alamos Scientific Laboratory, Los Alamos (1973).

[35] B. Rivière, M. Wheeler, *A posteriori* error estimates for a discontinuous Galerkin method applied to elliptic problems, Computational and Applied Mathematics 46 (2003) 143–163.

[36] C.-W. Shu, Discontinuous Galerkin method for time-dependent problems: Survey and recent developments, in: X. Feng, O. Karakashian, Y. Xing (eds.), Recent Developments in Discontinuous Galerkin Finite Element Methods for Partial Differential Equations, vol. 157 of The IMA Volumes in Mathematics and its Applications, Springer International Publishing, 2014, pp. 25–62.

[37] Y. Xing, C.-S. Chou, C.-W. Shu, Energy conserving local discontinuous Galerkin methods for wave propagation problems, Inverse Problems and Imaging 7 (2013) 967–986.

[38] Y. Yang, C.-W. Shu, Analysis of optimal superconvergence of discontinuous Galerkin method for linear hyperbolic equations, SIAM Journal on Numerical Analysis 50 (2012) 3110–3133.

[39] Y. Yang, C.-W. Shu, Analysis of sharp superconvergence of local discontinuous Galerkin method for one-dimensional linear parabolic equations, Journal of Computational Mathematics 33 (2015) 323–340.

Department of Mathematics, University of Nebraska at Omaha, Omaha, NE 68182, USA
E-mail: mbaccouch@unomaha.edu